A Case Study on Computational Fluid Dynamics Analysis of Micro-MIM Products

A Case Study on Computational Fluid Dynamics Analysis of Micro-MIM Products

Ian Andrews*, Kazuaki NISHIYABU**and Shigeo TANAKA***

ABSTRACT

Many people are familiar with computational fluid dynamics studies for plastic injection molded parts but little study has been undertaken in the field of micro metal injection molded parts. Micro metal injection molding (MIM) is a relatively new technology and many advances are progressing in production methods that increase accuracy and applicability of its use. Computational fluid dynamics studies of such methods can assist in furthering the advancement of this technology and can provide valuable information to manufacturers and consumers alike. A study on two micro-MIM manufactured test parts was done using Moldex 9.0 CFD and Rhinoceros 4.0 (with Moldex3D-Mesh plug-in software) Modeling software. The methods for realizing some common problems unique to micro-MIM analysis were proposed and applied to two micro-size MIM parts to find suitable process conditions in this paper. The results of this study were used to check for production viability and to improve the design of the test parts for possible future production. An ideal set of process conditions and assumptions was found for MIM CFD analysis performed in Moldex 9.0.

Key Words: micro metal injection moulding, computational fluid dynamics, production viability, micro gear

1. Introduction

Computational Fluid Dynamics (CFD) is the science of determining a numerical solution to the governing equations of fluid flow whilst advancing the solution through space or time to obtain a numerical description of the complete flow field of interest. CFD analysis consists of 3 main stages; Modeling and Meshing, Pre-Processing and Post-Processing. Each stage can be further split down into smaller sections. Modeling is the first stage that is undertaken with all CFD processes. This involves making 2D or 3D models of the geometry of the areas where the fluid flow analysis is required. For injection molded parts, this usually consists of models of the part, its mold and the cooling arrangement with the mold. After modeling the geometry of the required areas, these areas are required to be split into many small areas called meshes. The many complicated equations involved in CFD are solved in each of the many small areas throughout the geometry and flow properties can be derived from the results. There are many types of mesh, each suitable for various geometries or analysis methods. Pre-processing involves using the models and meshes created and inputting the desired material properties, flow properties, temperatures, process durations etc. For injection molding analysis, the injection machine properties such as injection pressure and packing length etc are often specified. The computation methods are also set in this stage. The type of mathematical solver, desired accuracy and various assumptions and simplification can be set here. Once all the properties and conditions are set the CFD analysis can be started. Post-processing is the final stage and is undertaken after the CFD analysis has finished obtaining a solution. In this stage the flow properties can be analyzed and various images, graphs and data can be seen. This data can be used as a qualitative tool for discarding (or narrowing down the choices between), various designs. Designers and analysts can study prototypes numerically, and then test by experimentation only those which show promise.

Whilst CFD is a very useful tool, CFD is not yet at the level where it can be blindly used by designers or analysts without a working knowledge of the numeric involved. Despite the increasing speed of computation available, CFD has not yet matured to a level where it can be used for real time computation. Numerical analyses require significant time to be set up and performed and have varying degrees of accuracy depending on flow properties and settings. CFD is an aid to

Received on 8th Aug. 2009

* Dept. of Industrial Systems Engineering : Mechanical Systems Course, Former lecturer

** Dept. of Industrial Systems Engineering : Mechanical Systems Course, Associated professor

*** Taisei Kogyo Co, LTD., President

other analysis and experimental tools like wind tunnel testing, and is used in conjunction with them. In particular, CFD analysis for micro injection MIM parts has not been undertaken to a great degree due to unreliable accuracy and computational resource difficulties but will become increasing useful as production and computer technology advances. CFD analysis alone cannot be relied upon to provide all the information for the optimal process conditions and methods, but it can simplify the process greatly.

2. Analytical Procedure

For this study two micro-MIM test products were analyzed using Moldex 3D v9.0 and Rhino modeling software v4.0. The procedure for CFD analysis is Moldex 3D and Rhino can be split into 4 main sections; Modeling, Meshing, Pre-processing and Post-processing.

2.1 Modeling The models used in the analyses were created from blueprints and engineering drawings in Pro-Engineer and imported into Rhino 4.0 in IGES file format. The geometries of the analysed parts are shown in Figure 1. The first part was dubbed 'Shikaku', and is a micro-sized MIM part. The size of the part is roughly a 14.55mm square with a 7.65x10.85mm rectangular hole in the centre, a groove cut into the surface surrounding the hole, and 4 tapered holes of 0.2mm diameter on the top surface. The part is also very thin, with a thickness of 0.4mm and 0.2mm in the groove region. The cubic capacity of the cavity is less than $0.05cm^3$. The second part is a micro-sized MIM gear with the diameter of the addendum circle being 1.12mm, depth of 0.8mm and a central shaft hole with diameter 0.42mm. The cavity cubic capacity for this part is approximately $0.0005cm^3$.

Extremely small characteristics of the geometries, such as minor tapers and chamfers that would have had little effect on the CFD results were ignored for simplification. After importing the IGES files from Pro-E to Rhino, they were checked for anomalies and to ensure they were enclosed 3D models with no defects. Next, basic initial runner systems were modelled and attached to the cavities. Both parts were non-finalised test products and as such had no runner size/shape, gate location or cooling system associated with them. Various runner types and gate locations were tested before settling on optimal specifications for each model.

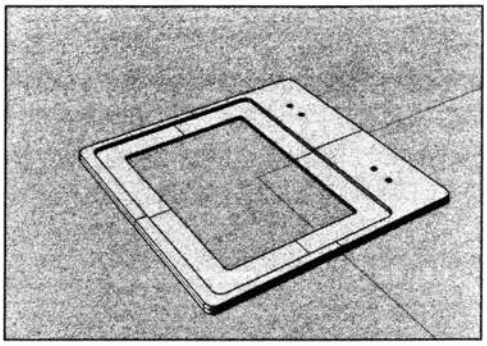

(a) Shikaku

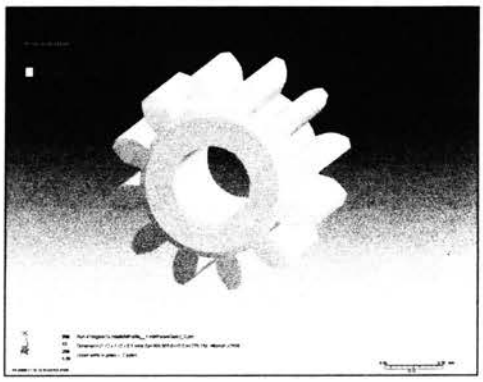

(b) Micro-gear

Figure 1 The geometry of the micro-parts

2.2 Meshing The cavities were checked again before meshing procedures were applied. Before meshing, nodes were assigned to all edges of the models, and in increased density in smaller, thinner sections of the cavity. This was done to ensure a reasonable element count across the section of the part, which affects the resolution and accuracy of the final results derived from the analysis. Initially a standard tetrahedral mesh was applied to the cavities, holes in the mesh were repaired and bad elements were fixed. After the surface cavities were meshed, the 3D runner meshes were created automatically using the function in Rhino, which forms prism meshes for reduced computational load and speed. Both meshes were checked for connectivity, then the 3D cavity mesh was generated and its elements were auto-fixed to remove poor elements. In all cases the total model element count was kept between 0.5-0.8million so many iterations of analysis could be performed with suitable speed and accuracy. The final meshing stage involved creating a mold-base face model which was cuboids surrounding the model and runner meshes. This mold-base face was also meshed using the auto function in Rhino, and was used to represent the mold in the analysis. In total, the cavity meshes and mold base meshes included approximately 1.0-1.2million elements. The complete 3D models were then exported to Moldex 3D v9.0 for analysis.

2.3 Pre-processing and Materials In the pre-processing section, the model, process conditions and computational solver conditions are set. A new project file was created in Moldex v9.0 for each model as shown in Figure 2. After the model was selected for analysis, the material used was specified. The material used in this study came from empirical data of material properties of Taisei Kogyo's MIM material, SUS316L 65:35 [1]. MIM material is a polymer of metal powder and a binding element comprised of waxy plastics. The metal powder molecules form an isotropic matrix inside the binder, which is removed at a later stage, so that only metal remains forming a tough part with good material properties. Whilst the material for the analysis had the material properties of MIM material, it is not currently possible to accurately model the all of the complex flow characteristics of MIM material, such as layer slip, compressibility and jetting. The material in the analysis had similar flow characteristics to that of a heavy plastic. After the material was set, the process conditions were set. In Moldex there are three setting types for the process conditions, two machine interface types and CAE mode. Most commercial injection-molding CFD programs cannot accurately model micro-parts using standard machine settings as they have unsuitable values for shot weights and flow rates etc.

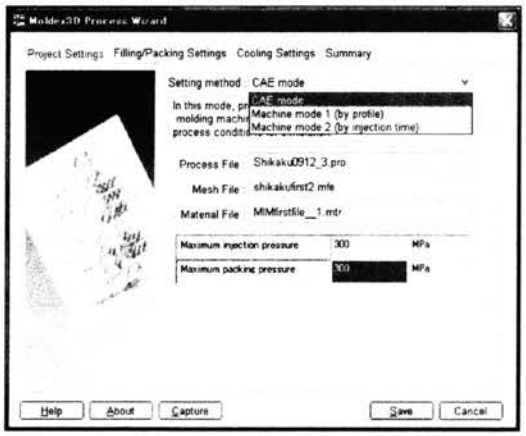

Figure 2 Project settings in the Process Wizard

In this study CAE mode was used for analysis as there was no empirical data available for process or machine settings. Initial tests showed default values for injection time and other criteria were unsuitable. Analyses using various speeds and pressures were performed until reasonable realistic results were obtained. A filling time of 0.1seconds was used for all models, along with a VP Switch-over of 99.5% and a packing time of 3 seconds. All other process conditions were used at default values. The final pre-processing stage was to set the computational solver method and assumptions. An Enhanced-P solver was used for all analyses. In the Advanced tab, the flow solver time-step was reduced from 1 to 0.1 to provide a better resolution at the cost of processing speed. In the Criterion for Stopping Calculation section, the 'exclude runner volume' box was checked as micro-parts are often much smaller compared to runner volumes than macro-size parts. After all process conditions were set and checked, the analyses were run using default settings for full run.

2.4 Post-processing The post-processing stage involves viewing and interpreting the results from the analysis. Upon completion of the calculation, the results for each model and process condition sets were checked. Each solution was checked for temperature, pressure, shear stress and shear rate and volumetric shrinkage. In the case of short shot or other errors such as hesitation, unacceptable shear stresses or over packing, the problem areas were identified and fixed before performing another analysis run. When process conditions or other settings were greatly changed, the calculation was performed in a separate Run within the same project for easy comparison between results. In this method, each model ran iterations of various conditions and settings until suitable results were obtained. Unique problems associated with micro-parts and their analyses were identified and rectified.

Many various parameters were investigated. First, the 'Shikaku' model will be used to illustrate some points of interest. The Shikaku model was difficult to solve as usually very thin parts can be difficult to manufacture by standard injection molding techniques and care must be taken when planning the molding conditions and gate locations. As an initial test, a standard side-gate into the part was modeled as shown in Figure 3(a). The runner used incorporated two cold-slug wells that closely resemble those present in experimental manufacture testing. The gate was chosen to be on the edge of the part closest to the 4 small holes as this is the largest area of the part and provides fairly unrestricted flow from the gate. The model was initially meshed with a standard tetrahedral mesh. The first plot to be checked in the post-processing stage is always the melt-flow front. Incomplete filling (or short-shot) is one of the most common problems in injection molding and is caused by a number of reasons as shown in Figure 3(a). The melt-flow front distribution will display any case of incomplete filling. By comparing the flow front animation to the graph of sprue pressure vs. time, the pressure loss due to certain features can be determined as shown in Figure 3(b). The flow progression through the cavity can be viewed by animation and critical areas such as voids and which areas fill last are easily seen. The effects

on the flow of cavity features like holes or thin channels can also be checked. This is useful when rectifying short-shot problems or when redesigning model and runner geometries for optimal flow conditions. The sprue pressure graph in Figure 3(b) shows that there is a peak in pressure loss caused by the cold slug well, followed by the large peak just after the slug well. These two losses account for a large percentage of the pressure drop and as a result, there is insufficient pressure to ensure complete filling in this case. This was caused by flow reversal from the slug well affecting the incoming flow, causing compression. Compressibility of material is not considered in Moldex3D yet. This shows that there is no need to accurately copy the runner shape used in manufacturing processes as this can adversely affect analysis results. A simplified runner will circumvent these errors and provide better results. This is especially important in micro-analysis as the runner size is often much smaller and more prone to such errors. In manufacture, complex runner shapes are often difficult to produce and realistically simple geometries would be used whenever possible. The melt-flow front also is related to where weld lines appear in the cavity. Weld lines form in cavities where two flow fronts meet and change direction. Such areas often do not have smooth unidirectional flow and material properties suffer in those regions.

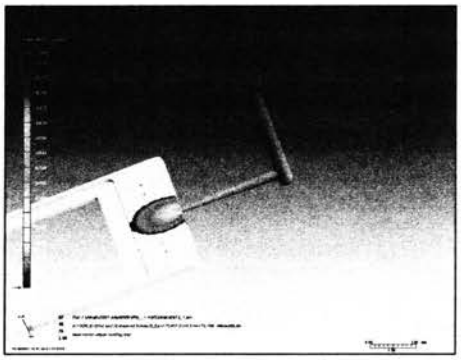

(a) Short shot

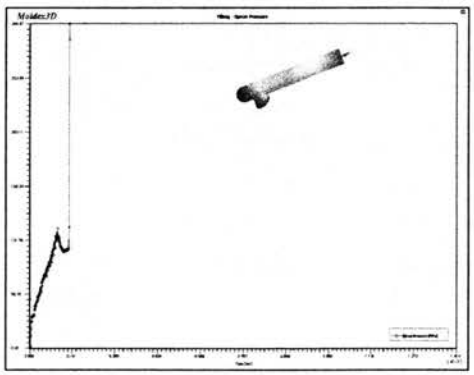

(b) Sprue pressure graph showing pressure losses

Figure 3 The initial test with cold-slug gate in the runner

Weld-lines in functional areas such as hinges or load centers drastically reduce the lifetime of parts and so should be confined to non-critical areas of the part whenever possible.

As can be seen in Figure 4, the flow pattern associated with this gate will form a weld line on the far side of the hole and will lead to weakening of this area of the part.

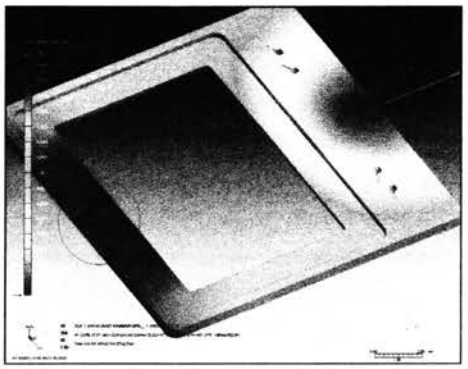

Figure 4 Weld Lines form in the circled location. This area would be weaker in comparison to the rest of the part

For micro-MIM analysis, the most important solution parameters were the plots of temperature, shear stress, shear rate and volumetric shrinkage distributions. By utilizing the Results Advisor option in Moldex 9.0 as shown in Figure 5, suggested values of each parameter were obtained as used as a base to check if solution were accurate or not. In collusion with the Results Summary wizard, which alerts the user of problem areas in the flow, accurate solutions for each model were achieved by manipulating the settings and solving in an iterative manner.

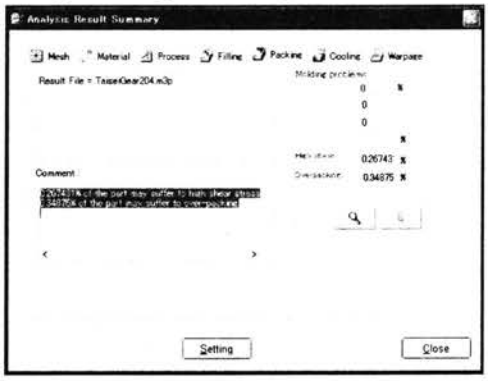

Figure 5 The result summary window from Moldex 9.0

Shear stress is one of the main sources of residual stresses in molded parts as shown in Figure 6. If the shear stress is not distributed evenly it can cause dimensional problems during and after the filling stage. If the shear stress is too high, stress-induced problems may also occur in the part, such as flow hesitation and burning out of the material. According to the results advisor in Moldex, the shear stress should be controlled to be less than 1MPa for most analyses.

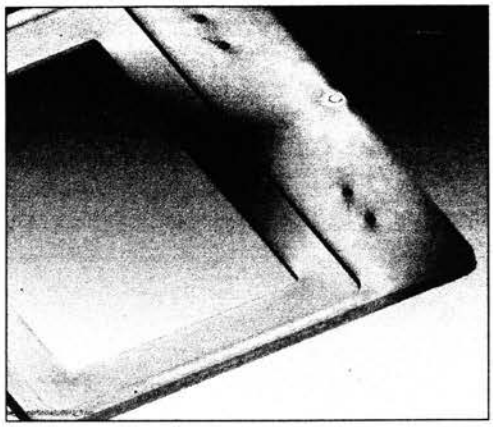

Figure 6 Shear stress during filling. The areas on the sides of the hole show very high stresses which would lead to problems.

Figure 7 Shear rate during filling. The areas on the sides would be subject to high viscous heating amongst other problems.

Shear rate is the rate of shear deformation of the material during flow as shown in Figure 7. A higher rate of shear indicates a higher rate of deformation, that is, the molecule chains in the polymer were deformed rapidly and had no chance to relax or recoil. Shear rate is related to the velocity gradient of the flow and the molecular orientation of the material. If the shear rate is too high, molecular chains can be broken and the strength of the product will be decreased. Viscous heating of the material through shear will also be present. From the Results Advisor, the recommended value for this shear rate usually falls below 10000 1/second, but for micro-parts this value is difficult to obtain in most cases. Moldex 9.0 performs best under standard machine settings for most values, such as filling time, which has a minimum filling time of approximately 0.05 seconds. If using a default machine filling time for a micro-cavity, the filling time would be in the order of 0.0005 seconds which causes very high velocities in the cavity leading to a number of errors such as high shear stress and shear rates. In CAE settings, users are able to more realistic values for filling time. In general, in all observed micro-MIM analyses shear rate was higher than that usually observed in standard macro-size cavities. In this study a shear rate value much higher than 50000 1/second was assumed to be undesirable. This value was derived from average shear rates in micro-cavities that had no warning errors from the Results Summary Wizards and had good, balanced flow profiles. Values for max shear rate will vary with material properties but in general, high shear rate leads to burning out of the material, pressure loses and hesitation in thin walled parts and should be reduced whenever possible.

The temperature distribution helps to show the effects of heat transfer throughout the part and is of great use when designing cooling channels, specifying cooling temperatures and times, and identifying areas of viscous heating from shear, or flow freezing leading to hesitation as shown in Figure 8. In this study, no cooling was specified but could be easily designed from the temperature distribution is required at a later date. The main use of the temperature distribution was to identify areas inside the cavity where calculation was prematurely stopped. In most standard analyses, the filling calculation is stopped when approximately 99% of the cavity is filled. This is in order to prevent the sharp pressure increase present during the final 1% from adversely affecting the simulation. As the size of micro-parts cavity is very small compared to the runner, this final percentage often is a substantial part of the cavity and solver settings must be changed to reflect this or an area in the cavity will appear where the results cannot be read. When setting the computation parameters, the "Exclude runner volume" box should be ticked in the "Criterion for Stopping Calculation" area in the advanced settings tab. When viewing the temperature distribution, the areas of 'no calculation' are easily seen. These areas appear due to many complex reasons, such as poor resolution, time-step being too large and due to a solver error in Moldex 9.0, resolved in Moldex 9.1.

The volumetric shrinkage at 'end of packing stage (EoP)' is also important for all injection molding analyses as shown in Figure 9. If the distribution of shrinkage is imbalanced inside the cavity it is likely the part will warp and lose functionality after ejection from the cavity. Also, the degree of shrinkage is important. An often-used value for reasonable shrinkage is 4%. If the shrinkage exceeds 4% by a large amount shrinkage of the part occurs to a great degree and the post-ejection shape cannot

be controlled with any accuracy. The volumetric shrinkage is dependant upon the thickness of the part, the temperature of the material and the cooling rate and distribution inside the mold. In the case of the test parts in this study, no cooling channels were present so only the balance was analyzed.

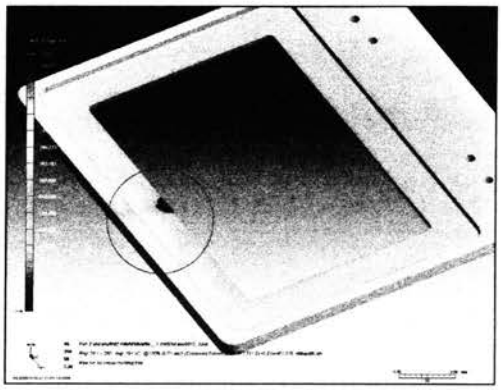

Figure 8 Temperature distribution. The region in the circle is the area of no calculation.

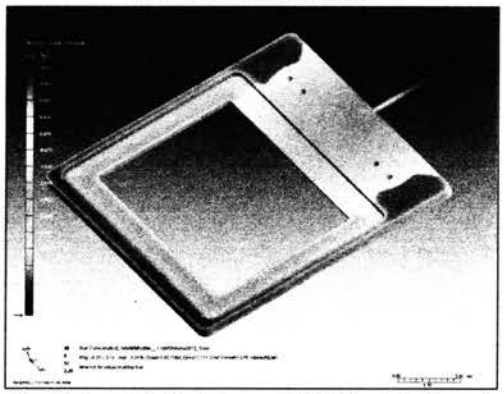

Figure 9 Volumetric Shrinkage at EoP. The imbalance leads to warpage of the part.

3. Results and Discussions

3.1 Determining micro-analysis process conditions

Firstly, an ideal set of process conditions for micro-size cavities in Moldex 9.0 was investigated. The model of the Shikaku test part was used for the investigation. After performing analyses on the basic Shikaku cavity many areas with poor flow properties were identified due to the presence of the large hole in the centre of the part. There were no ideal gate locations that would alleviate the problems. An alternative geometry for Shikaku was modeled as shown in Figure 10. In this model, the central hole was filled in and used as a location to place the gate. The thickness of this region was also increased as to provide a more ideal flow pattern from the gate. With this geometry, the manufacturer would have to cut the 'filled in' section from the part after manufacture which would lead to further costs.

A series of tests were performed on the new model with varying filling times, flow rates, injection pressures and packing pressures until error-free accurate results were obtained. The testing parameters were shown in Table 1. The flow rate was set at a percentage of maximum possible. The injection pressure and packing pressure are set at a percentage of maximum pressure, which was set at 300MPa in CAE Mode.

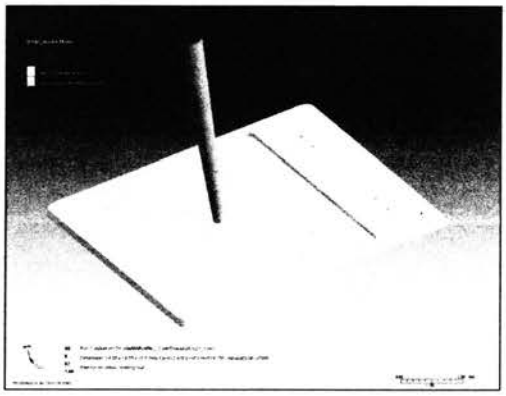

Figure 10 The alternative geometry for the part, gate location and runner.

Table 1 Testing parameters

Run No.	Filling time (s)	Flow rate (% of max)	Inj. Pres. (%)	Pack Pres. (%)	Shear Rate OK	Shear Stress OK
1	0.00242	50	70	70	No	No
2	0.05	20	40	50	No	Yes
3[a]	0.5	20	40	50	Yes*	No
4	0.1	50	70	70	Yes	Yes
5[b]	0.1	50	70	70	No	Yes

a) In Run 3, short shot occurred therefore all process settings were deemed unsuitable despite falling within acceptable ranges for some parameters. b) In Run 5, a simplified geometry for the cavity was used.

(1) Run 1

Run 1 was performed at standard default settings in CAE mode. The filling time is much faster than that of standard analyses. As can be seen in Figure 11, the new geometry has a more balanced flow profile and no weld-lines in critical locations, but the shear rate was still unsuitable, with a max value exceeding 500000/s. The shear stress also greatly exceeded acceptable limits.

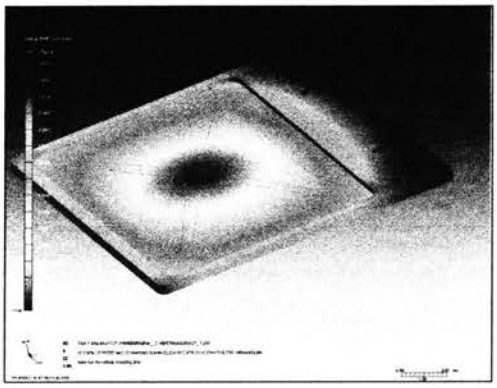

(a) Melt Flow Front

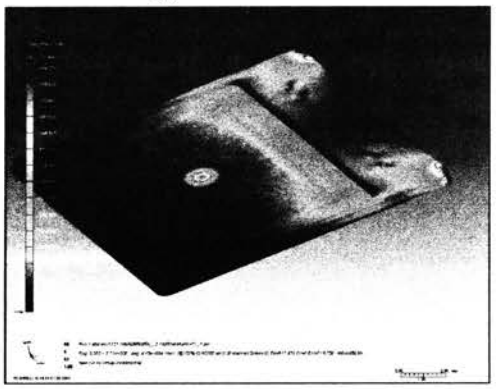

(b) Shear Rate

Figure 11 The Melt Flow Front and the distribution. The shear rate is still in the order of 10 times the recommended level.

(2) Run 2

The results showed that although the shear stress was now within acceptable values, the shear rate was still too high as shown in Figure 12. The shear rate is much improved but still high with critical areas having values between 20000 to 50000/s. Further improvement was investigated as shown in Figure 13.

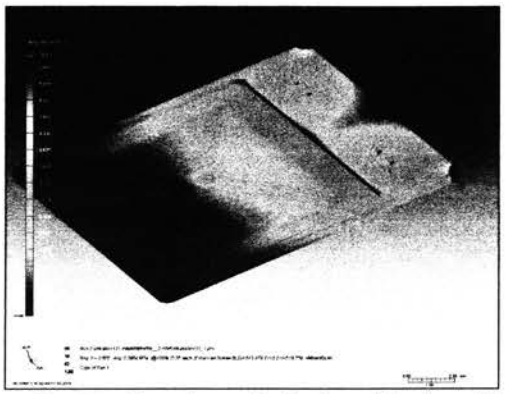

Figure 12 The Shear Stress distribution. All values of shear stress fall under 0.6 MPa.

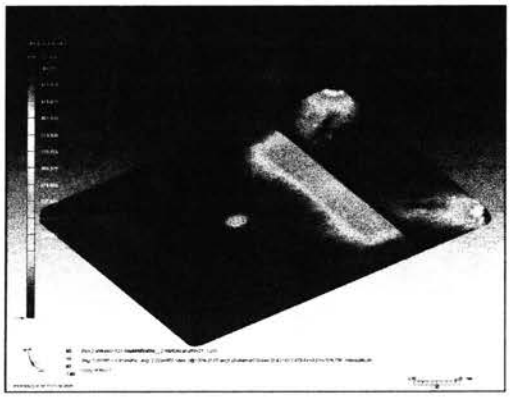

Figure 13 The Shear Rate distribution. Values range between 20000-50000/s

(3) Run 3

The shear rate now fell within acceptable limits but the shear stresses were too high. The flow rate at this speed was too slow to completely fill the model before hesitation and short-shot occurred as shown in Figure 14.

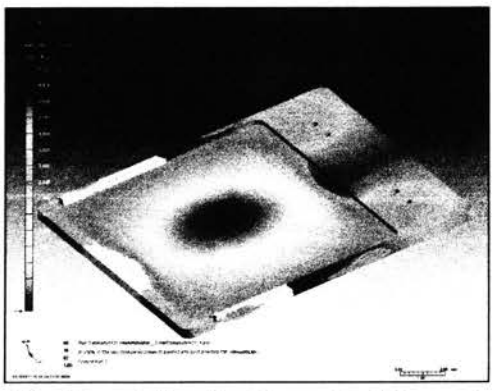

Figure 14 The melt flow front. Incomplete filling can be seen indicating short-shot.

(4) Run 4

With these settings the shear rate and shear stresses both fell within acceptable ranges as shown in Figure 15.

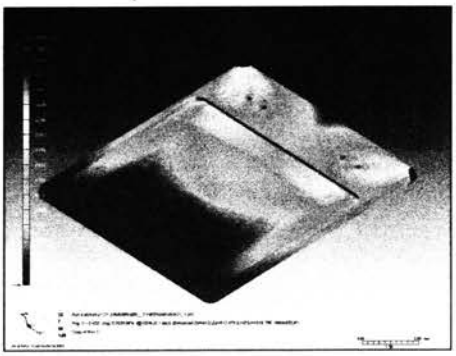

(a) Melt Flow Front

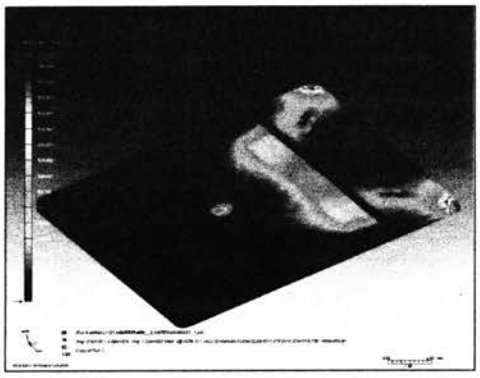

(b) Shear Rate

Figure 15 The Shear Stress and Shear Rate distributions. The critical areas of the part now have a value of approximately 0.4MPa and 7000-30000/s respectively.

The volume shrinkage distribution of the alternative shape was also investigated once the process conditions were satisfactory. The volume shrinkage can be seen below in Figure 16, and it can be seen that it is much more balanced and less likely to have a large degree of warpage.

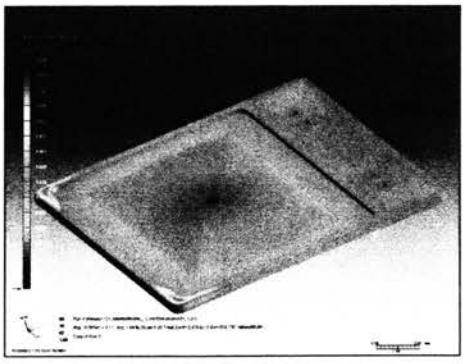

Figure 16 The volume shrinkage distribution of the alternative geometry.

In this model, the thin parts of the model are those subjected to the highest shear stress and are the restricting factor of this geometry. There is also a degree of sudden expansion occurring from the flow from thin regions to the thicker regions. This could be improved on by rounding corners and/or increasing the taper between the surfaces.

The thickening of the region where the gate was located was in order to prevent shear problems due to sudden expansion and friction. The distribution of shear rate near the gate is shown below in Figure 17.

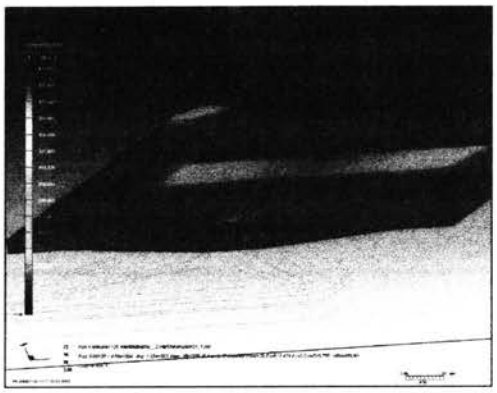

Figure 17 Shear Rate Distribution of Run 4. Showing the cross-section near the gate and the relatively low shear rate.

(4) Run 5

A final analysis was run using a model with no central hole as shown in Figure 18. This geometry would be less desirable for manufacture as it would require a minimum of two further processes to achieve the final product shape; cutting of the central hole, and pressing of the area surrounding the hole to the specified thickness.

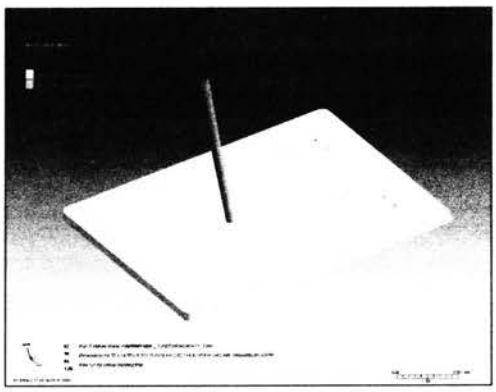

Figure 18 Model with no central hole

The results show that this model has the most balanced melt flow front and volumetric shrinkage, as seen in Figure 19.

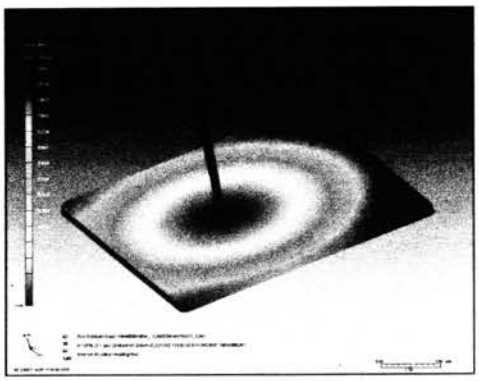

(a) Melt Front Flow Time

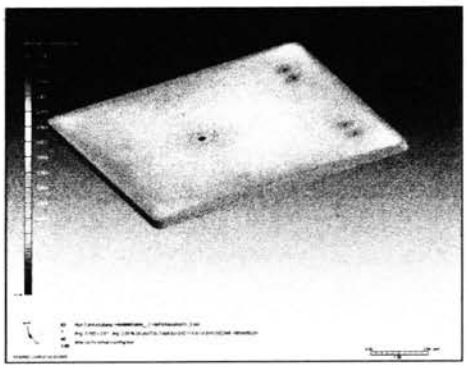

(b) Volumetric shrinkage

Figure 19 Melt Front Flow Time and Volumetric shrinkage at End of Packing phase

An interesting thing to note was this geometry also had an unsuitable shear rate when using the previously determined process conditions. The shear rate near the gate was very high due to the perpendicular flow from the gate, causing high friction. The cross-section of the shear rate at the gate is shown in Figure 20.

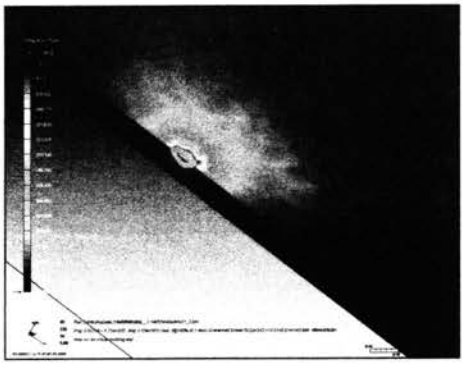

Figure 20 Shear rate distribution at the gate location.

In order to resolve the shear rate, the input velocity must be decreased, but care must be taken not to cause a short-shot as in the case of Run 3. In general, gating perpendicularly into thin regions should be avoided when possible. The best set of process conditions for this model came from Run 4. The filling time was found to have more effect on the results than the other settings. Moldex 9.0 does not handle very fast filling times well. Depending on the size of the cavity, filling times should be kept with 0.5-0.05seconds when possible. Shorter filling times result in shear problems, and longer times can result in short shot due to the rapid cooling of flow due to heat transfer, which is much more significant in micro-analyses.

3.2 Improving accuracy of micro-analysis. Using the process conditions derived previously, tests were run on the micro-gear cavity shown in Figure 21 in order to reduce errors and anomalies in micro-analyses and to improve accuracy. Varied geometrical models with different runner/gate locations shown in Figure 22 were analyzed.

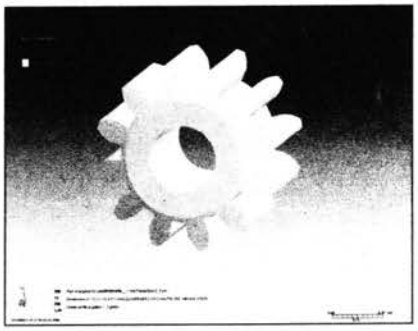

Figure 21 Geometry of the micro-gear part.

(a) Model 1R2G

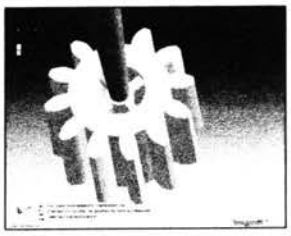

(b) Model 1R4G

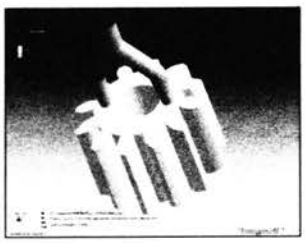

(c) Model 2R2G

(d) Model 3R3G

Figure 22 Geometry of the runner/gate locations.

The models were initially meshed with a standard tetrahedral mesh. The material used in this study came from empirical data of material properties of Taisei Kogyo's MIM material, SUS316L 65:35 [1]. The process conditions from Shikaku Run 4 were checked for suitability for this cavity and tested prior to the investigation. In all analyses of the models, areas of no

calculation could be seen spread throughout the cavity (Figure 23), as in the case of the area of last fill in Shikaku, seen on the temperature distribution (Figure 8). A detailed description of all results can be found in the detailed Micro-Gear report [2]. As the cubic capacity of the micro-gear is much smaller than that of the Shikaku model, more care must be taken with accuracy or small assumption errors can greatly affect the outcome. For the Shikaku analysis, the area of no calculation was not in a critical region and had negligible affect on the outcome. In the micro-gear analysis, the same problems had a large affect and affected the shear stress distribution as shown in Figure 23.

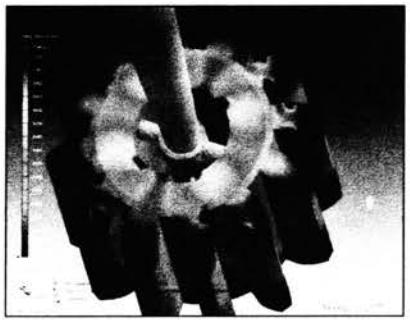

(a) Model 1R2G

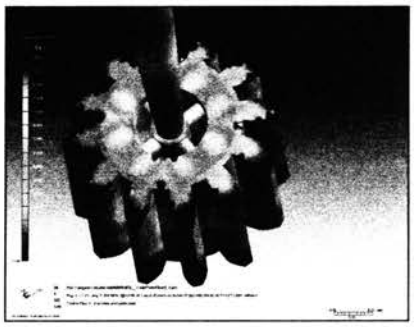

(b) Model 1R4G

Figure 23 The shear stress distributions for the micro-gear tests. Many small areas of no calculation are present.

A variety of solutions were applied to attempt to remove this inaccuracy. Initially, the problem was thought to stem from an imbalance in the flow profile of the models tested. A final runner/gate model was created and tested. In this case a 'cap' was created on the top surface of the gear and the gate was located onto the cap as shown in Figure 24. This made it so the entire top surface of the gear acted as a gate and flow could be more symmetrical. The entire cap and gate location would have to be removed after manufacture by a cutting method as shown in Figure 25. It is shown in Figure 26 that the runner cap model provides a much more symmetrical flow front and resulting post-processing material conditions.

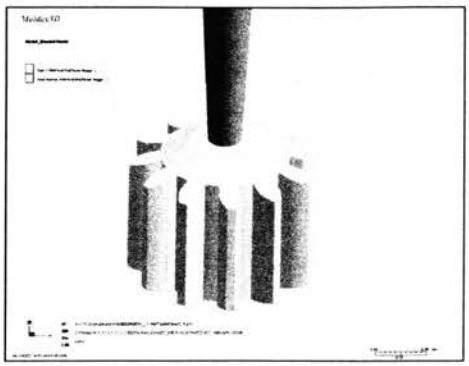

Figure 24 The runner cap shape and location.

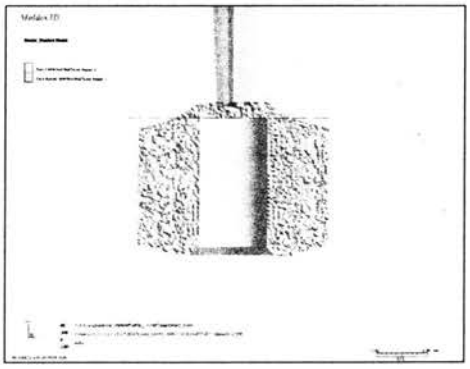

Figure 25 A cross-sectional view of the runner cap model and mesh elements. The cap area above the red line must be removed after manufacture. The internal tetra mesh elements can be seen.

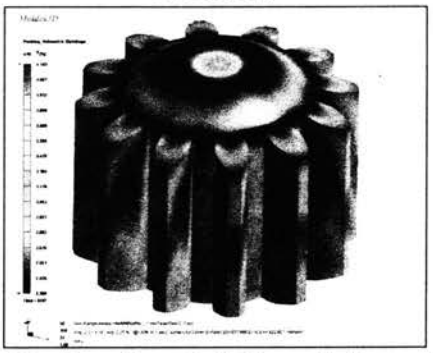

Figure 26 The volumetric shrinkage distribution for the capped model. The shrinkage is symmetrical and more balanced than previous models.

Despite being symmetrical and having a smooth flow profile, the no calculation error was still present (Figure 27) and greatly affected the results. Many causes for these errors were investigated and the results are explained below. Firstly, a common cause of such areas is due to the solver resolution being too low. If the time-step of the computational solver is too large, there will be too few solver iterations for the results to show small changes. To increase the resolution, the time-step must be decreased, which enables the computation to solve at a

greater number of times per second. In the advanced settings window of the computational parameter window, the default solver time-step is set to a value of 1. Various time steps were tested ranging from 0.02 to 1. By decreasing the solver time step however, the analysis time is greatly increased. A balance must be found for efficient time and resource usage. Initially with the default time step of 1, the analysis took approximately 10 hours on the computer used. At the lower end with a time step of 0.02, the analysis took over 3 days to complete. Whilst the resolution had improved and area regions decreased such a level is rarely required. A time step of 0.1 was tested and this provided better resolution without sacrificing too much time, the analysis took about 20 hours to complete.

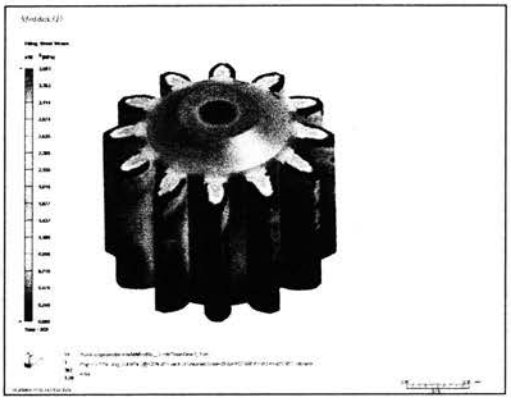

Figure 27 The shear stress distribution for the runner-cap model with BLM in Moldex 9.0.

The results were more accurate but the problem errors were still present. The temperature distribution was used to display the areas of no calculation clearly. Secondly, the effect of the standard tetra mesh elements beginning to become inaccurate for micro-CFD models was investigated. In injection molding analysis, the element layer count across the part thickness direction is very important. This is because the element layer count determines the resolution of the analysis result. For example, in the case of the temperature distribution shown in Figure 28, the temperature changes rapidly on the part's surface due to a combination of shear heating and contact with the mold causing heat transfer. With low resolution, such changes cannot be seen and inaccuracy develops. When creating standard tetra meshes, the element count across the part cannot be controlled by the user, thus the analysis cannot provide correct temperature distribution in poor quality mesh regions. However, accurate results can be achieved by using a different meshing method. For complex flow profiles or unusual material properties, a hybrid mesh often provides the best results although hybrid meshes can be very difficult and time-consuming to create. A better solution is to use a Boundary Layer Mesh, which is a simplified hybrid mesh which can be created automatically in Rhino 4.0. A boundary layer mesh, or BLM, consists of the standard tetra mesh with a thin layer of prism mesh on the outer surface as shown in Figure 29. BLM meshes increase the element layer count and therefore the resolution which, in the case of micro-injection molding analysis, is doubly important. The shear heating phenomena can be simulated more accurately. Further, the analysis results of the filling pattern, pressure profile and so on, can be predicted more accurately as well.

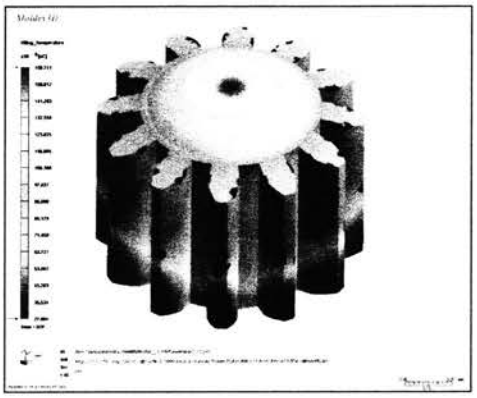

Figure 28 The temperature distribution for the runner cap model using tetra mesh in Moldex 9.0.

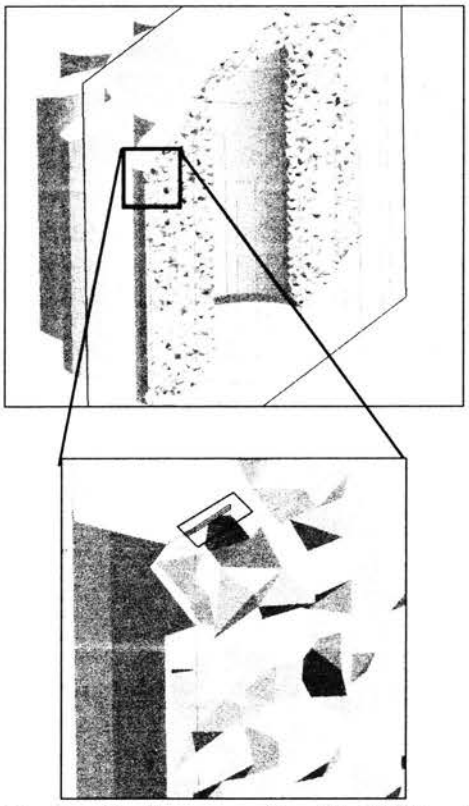

Figure 29 Showing the cross-section of the BLM mesh. Two very thin prism elements can be seen outside the tetra elements.

An analysis of the part using the original process conditions and a BLM mesh was performed and the temperature distribution was checked for anomalous areas. The result is shown in Figure 30.

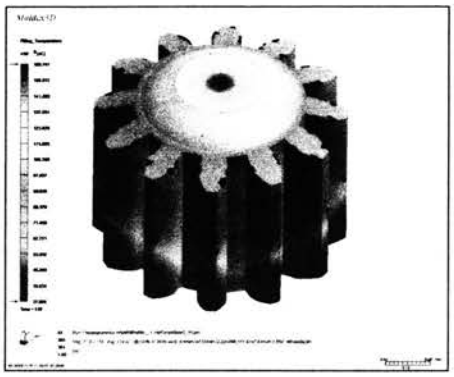

Figure 30 The temperature distribution for the runner cap model using BLM mesh in Moldex 9.0

The problem still persists for a BLM mesh in Moldex 9.0. All the parameters and settings were checked and a warning message W1502 located in the packing log file was investigated as shown in Figure 31.

```
-------------------------------------------------
  No  Time(sec)  Pres(Mpa)  Fill(%)    CPU(sec)
-------------------------------------------------
  51    0.781      42.51      100.0       5516

!!! WARNING  W1502 : ( Moldex3D/Solid-Pack: R9.0 Build 90696 )

The melt temperature is too close to Tg of the material. This issue may induce
computational stability problems and lead to worse results. Because:
1. Tg of material may be too high. Please re-check the material properities.
2. The input of melt temperature may be too low.

  52    0.868      42.51      100.0       5626
```

Figure 31 The warning message W1502 in the packing log file in Moldex 9.0.

The cause for this warning is not known but in order to test if it had an effect on the result, one analysis was performed in the new Moldex 9.1, in which many small bugs have been fixed. The warning message was not present in the log file for the Moldex 9.1 analysis and the temperature distribution is shown in Figure 32.

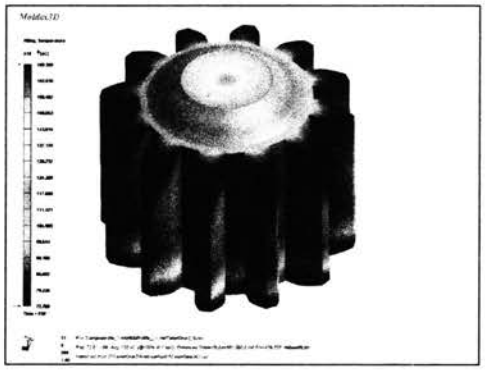

Figure 32 The temperature distribution for the runner cap model using BLM mesh in Moldex 9.1.

As can be seen, the distribution is smooth and there are no problem areas such as in figure 30. The resolution of this model and is still reasonably fast and easy to create. It is recommended that Moldex 9.1 should be used if problem areas persist, and all micro-size analyses performed in Moldex should use a BLM mesh where possible for improved accuracy.

4. Conclusions

Two micro-size MIM test parts were analyzed using Moldex 9.0 and Rhino 4.0. A series of suitable process conditions were devised for using in micro-analyses in Moldex 9.0. Common errors present in micro-analyses were identified and solutions were investigated.

(1) Filling time has a large effect when performing micro-analyses. Moldex 9.0 works best with filling times in the range of 0.05-0.5seconds.

(2) Extra care must be taken with runner shapes and gate locations in micro-analysis due to the exceptionally small and thin cavity shapes.

(3) Areas of no calculation are common in micro-cavities and present a substantial inaccuracy. These errors can be reduced by using a BLM with reduced time-step and preferably, Moldex 9.1.

5. Acknowledgments

The authors of this paper would like to thank Mr. Hisahiro Tanaka of Saeilo Japan Inc., Osaka, for providing his assistance with analysis methods and advice for both Moldex 3D and Rhino programs

6. References

[1] Julin Chiao, Polymer Property Analysis Report, MIM SUS316L 65:35. Serial No. 00362, Supplier – Core Tech, Material Code – TAISEI-1024, CAE Laboratory, Department of Chemical Engineering, National Tsing-Hua University, 19 Dec. 2002.

[2] Ian Andrews, Taisei Kogyo Report 2 – Micro-MIM gear Analysis, Osaka Prefectural Technical College, January 2009.